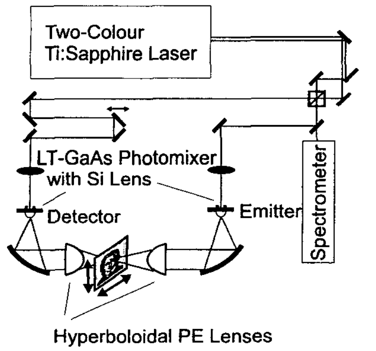

CFD1 Fig. 1. Set-up of the all optoelectronic cw THz imaging system.

mirror and then focused by a plano-hyperboloidal lens. Behind the focus the inverse set of optics is used to focus the THz beam onto the detector antenna. For THz imaging objects can be moved through the object on a meandering path. The system obeys a signal-to-noise ratio of 100:1 defined as the ratio of the mean amplitude versus its standard deviation. The plano-hyperboloidal lenses were manufactured in-house from high-density polyethylene and allow for very short focal lengths (here: 2 cm) while producing aberration-free foci. Moreover, such lenses have the additional advantages that they are relatively thin even for large apertures, and can be positioned easily because their principal plane is always at the lens apex. The spatial resolution obtained with this configuration is on the order of the THz wavelength.

We demonstrate cw THz imaging with complex sample and compare the results with images taken with a state-of-the-art pulsed system based on an Ti:sapphire amplifier laser operating at 1-kHz repetition rate.[5] The sample was a formalin-fixed, dehydrated and wax-mounted slice through a canary's head (see Fig. 2d). The size of the sample was 32 mm × 24 mm × 3 mm. Figure 2 shows logarithmic power transmission images taken both with the cw system at 1 THz (Fig. 2b) and the pulsed system at 1 THz (Fig. 2b). Both images consist of 3072 pixels, with a spacing between neighboring pixels of 0.5 mm. To compare the image quality, the relative power transmission for line scans at fixed y-positions is studied. The contrast achieved with the cw system compares well with that obtained using the pulsed system. In addition to the amplitude information, the relative phase of the cw wave at each pixel can be exploited for image formation as shown in Fig. 2c). Nearly all features observable in the power picture can be seen here as well. We acknowledge financial support by the Deutsche Forschungsgemeinschaft and by the EU project TERAVISION within the IST-framework

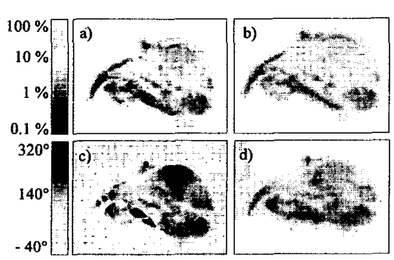

CFD1 Fig. 2. a) Cw THz image at 1 THz of a wax-mounted thin-cut canary's head; object size: 32 mm × 24 mm × 3 mm. Plotted is the relative power transmission. b) Corresponding pulsed THz image at 1 THz. c) Cw THz image obtained from the phase information at 1 THz. d) Photograph of the sample.

References

1. B.B. Hu, and M.C. Nuss, Optics Lett. **20**, 1716 (1995).
2. D.M. Mittleman, M. Gupta, R. Neelamani, R.G. Baraniuk, J.V. Rudd, and M. Koch, Appl. Phys. B **68**, 1085 (1999).
3. S. Verghese, K.A. McIntosh, S. Calawa, W.F. Dinatale, E.K. Duerr, and K.A. Molvar, Appl. Phys. Lett. 73, 3824 (1998).
4. F. Siebe, K. Siebert, R. Leonhardt, and H.G. Roskos, IEEE J. Quantum Electron. 35, 1731 (1999).
5. T. Löffler, T. Bauer, K. Siebert, H.G. Roskos, A. Fitzgerald, and S. Czasch, (submitted to Optics Express).

CFD2 **8:15 am**

Synthetic Phased-array THz Imaging

J. O'Hara and D. Grischkowsky, Department of Electrical and Computer Engineering and Center for Laser and Photonics Research, 202 Engineering South, Oklahoma State University, Stillwater, OK 74078, Email: ohara@thzsun.ecen.okstate.edu

Improvements in resolution are beneficial to any imaging system. Since they are usually incoherent, optical imaging systems infrequently utilize synthetic aperture and phased-array techniques to improve resolution. Imaging with coherent, broadband THz pulses, however, can benefit from these well-known techniques. Using these techniques, we demonstrate resolution enhancement in an established THz imaging system.

Figure 1a shows the plan view of the THz imaging system. The experimental arrangement is nearly identical to the one used in previous work[1] with two exceptions. First, the object can be translated in two dimensions. That is, it can be moved anywhere within the *xy*-plane, to which the optic (*z*) axis is normal. Second, this plane of motion can be rotated, or tilted, about the *x*-axis. Figure 1b illustrates the object's motion. In the normal configuration the object moves within the *xy*-plane. In the tilted configuration the object moves within the *xy'*-plane, which is the *xy*-plane rotated 15° about the *x*-axis. The fixed origin marks the (x = 0, y = 0, z = 0) position of the object for both configurations thereby providing an absolute phase reference. The motivation for the two configurations will become clear.

As in previous work, the object is scanned through the incident THz beam and the spherical mirror forms a real, one-to-one, diffraction-limited image, which is recorded one portion at a time by a fixed receiver. The object is a 1 mm diameter steel sphere which, when illuminated, can be regarded as a point source of THz. Therefore, the corresponding image represents the smallest pixel the THz imaging system can generate using the normal configuration.

To increase the resolution it is necessary to increase the size of the most limiting aperture in the system; in this case the spherical mirror. Since it is coherent, the THz imaging system can use phased-array techniques to accomplish this task. Therefore it is possible, by using two adjacent spherical mirrors and treating each mirror as a phased-array element, to effectively increase the aperture size and thereby increase the system's resolution in one dimension.

Figure 2a shows how such a 2-mirror system would appear if physically implemented. The image formed by the 2-mirror system can be synthesized by combining the two images formed separately by mirror 1 and mirror 2. To achieve this effect, the THz imaging system was used, once in the normal configuration and once in the tilted configuration of Fig. 2b, to generate two, coherent, diffraction-limited images shown in figure 3. In the first image (Fig. 3a), the object was scanned in the *xy*-plane. In the second image (Fig. 3b) the object was scanned in the *xy'*-plane.

Instead of physically implementing mirror 2

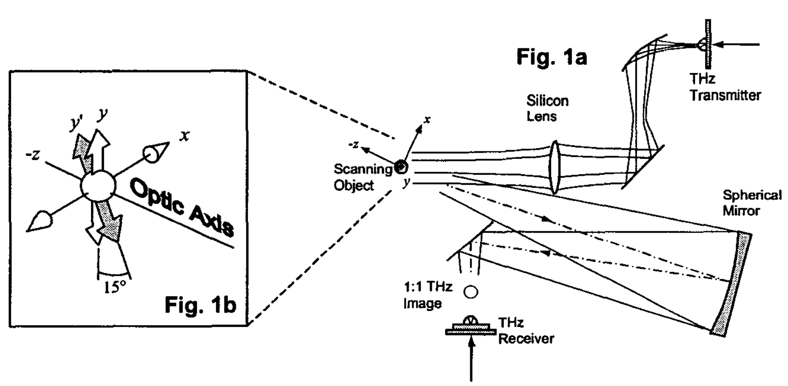

CFD2 Fig. 1. The THz imaging system, plan view, is shown in Fig. 1a. The object, a 1 mm diameter steel sphere, is mounted on a stealth-shaped paraffin holder, which is invisible to the system. The dash-dot line defines the system's optic axis. Fig. 1b shows a detailed picture of the object and its two planes of motion. The flat arrows lie in these planes of motion. Note that the view in Fig. 1b has been rotated relative to Fig. 1a.

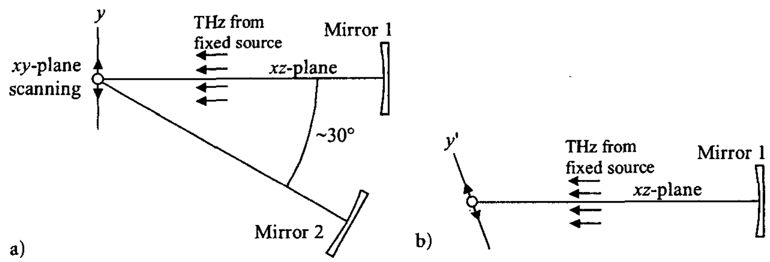

CFD2 Fig. 2. Shown in Fig. 2a is the physical manifestation of a 2-element, optical phased array with mirror separation equal to ~30°. In this 2-mirror system, the object scans in the *xy*-plane which is normal to the optic axis of mirror 1. However, this plane of motion is tilted ~30° off normal to the optic axis of mirror 2. Fig. 2b shows how mirror 1 is used to generate the image that mirror 2 would generate if it were actually implemented.

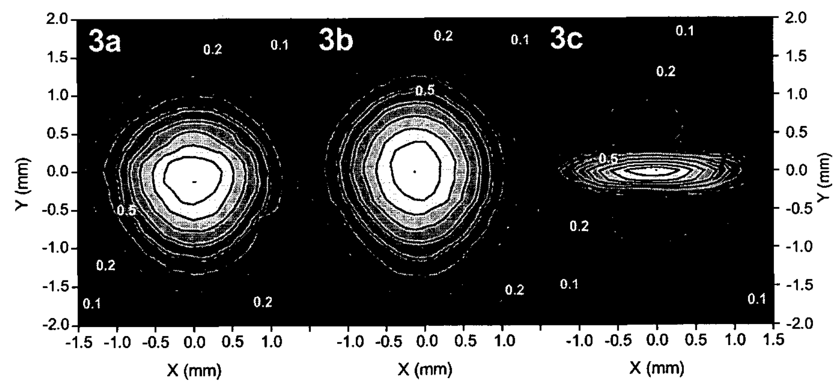

CFD2 Fig. 3. Single mirror images of the 1 mm ball at 0° and 15° orientations are shown in Fig. 3a and Fig. 3b. Fig. 3c is their direct superposition and shows the enhanced vertical resolution. All plots are normalized to unity and contour lines represent steps of 0.1.

to form the second image, mirror 1 was re-used. This was possible by leaving mirror 1 fixed but giving it the viewpoint of mirror 2. Figure 2b shows how mirror 1 can be given this viewpoint by tilting the scanning plane. Scanning the object in the *xy*'-plane (the tilted configuration) made it possible to obtain the same image mirror 2 would generate without ever physically implementing it. That is, by simply tilting the scanning plane about the *x*-axis, mirror 1 behaved as mirror 2.

One important point for our experiment is that the second mirror appeared to be located ~30° below the first, even though the scanning plane was only rotated 15°. This subtle point is a consequence of both configurations having the same fixed THz illumination source. The tilted configuration introduces phase changes as the object moves closer to and farther from the source (in the +*z* and –*z* directions respectively), when scanned along the *y*'-axis. If the object was self-luminous, this would not be a factor and the second mirror would appear to be located 15° below the first, as one would expect. Fortunately, the 30° apparent separation is actually beneficial because it creates a larger synthetic aperture thus improving resolution over the 15° case. Figure 3c shows the superposition of both images and the ~4× increase in resolution in the vertical dimension, where resolution is defined by the full-width-half-max measurement of the image. The horizontal dimension does not show any increase in resolution. These observations are in good agreement with theory and show the potential of high-resolution, phased-array THz imaging.

Reference

1. J. O'Hara and D. Grischkowsky, "Quasi-optic terahertz imaging", Opt. Lett. 26, 1918–1920 (2001).

CFD3 **8:30 am**

Towards an Apertureless Electro-optic T-ray Microscope

Tao Yuan,[1] Samuel Mickan,[1,2] JinZhou Xu,[1] Derek Abbott,[2] and X.-C Zhang,[1] [1]Department of Physics, Applied Physics and Astronomy, Rensselaer Polytechnic Institute, Troy, NY 12180, USA; [2]Centre for Biomedical Engineering and Department of Electrocal & Elctronic Engineering, Adelaide University, SA 5005, Australia; Email: Zhangxc@rpi.edu

Using the sub-wavelength aperture near field method, the resolution of THz image has been improved to much less than the wavelength or even to 7-μm[1,2] in last several years. However the transmitted power of this method is very low, and the detection antenna has to be very close to the aperture.[3] We demonstrate another kind of near field method: ultrafast laser is focused to a very small spot so that THz waves only generate in this region. The idea spatial resolution is close to the focus spot size.

The laser system is the Coherent Mira Laser with Pulse width ~100 fs and repetition rate of 76 MHz. We use objective lens to focus the pump beam on the EO crystal. The THz wave is measured using EO detection and a balanced detector.

First we measure the focus spot size of the laser in a 250 μm thick ZnTe crystal. For laser wavelength of 0.8 μm, the predicted spot diameter for a Gaussian beam is 2.55 μm/NA = 0.4 and 1.57 μm/NA = 0.65, which are very close to our measured values of 2.5 ~ 3 μm/NA = 0.4 and ~1.7 μm/NA = 0.65. The laser can be focused down to a spot size of 1.7 μm even after it in a several hundred μm thick media plate of high refractive index (ZnTe ~2.9). The proceeding data was obtained using a 20×/0.4 objective lens.

THz wave is generate in the whole beam region in the crystal, the spatial resolution is thereby restricted.[4] This problem is alleviated by using a very thin crystal to generate the THz wave. The generation of THz wave by thin crystal shows very different phenomenon at the focus point compared to a thick crystal. Figure 1 shows the THz peak signal of a 250 μm-thick ZnTe and a 16 μm-thick ZnTe crystal vs. the focus lens position. The pump power is 10 mw (after AO Chopper) for both cases. For the thick crystal the THz signal is reduced when the focus spot is in the crystal while for the thin crystal the opposite effect is seen and we see a strong peak of THz signal in the focus region. Figure 2 shows the THz waveforms of 10 mw-pump power at focus point

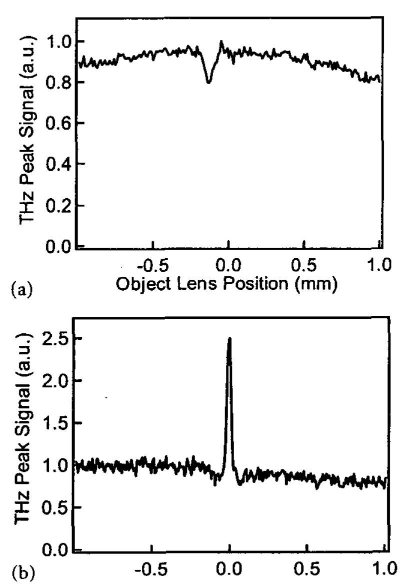

CFD3 Fig. 1. Peak THz signal of thick and thin ZnTe crystal pass through the focus region. (a) THz Peak Signal (a.u.) of a 250 μm ZnTe vs. Object Lens (20×/0.4) Position. (b) THz Peak Signal (a.u.) of a 16 μm ZnTe vs. Object Lens (20×/0.4) Position.